MAPPING THE GALAXY DISTRIBUTION AT LARGE DISTANCES[1]

CHRISTÈLE BELLANGER AND VALÉRIE DE LAPPARENT

CNRS, Institut d'Astrophysique de Paris, 98 bis, Boulevard Arago, F-75014 Paris, France

Received 1995 May 18; accepted 1995 October 3

ABSTRACT

We present the first results of the ESO-Sculptor Faint Galaxy Redshift Survey designed to study the large-scale galaxy distribution at large distances in the direction of the southern Galactic pole. The galaxy catalog is based on deep multicolor CCD photometry. To date, 353 galaxies with $R \leq 20.5$ have a reliable redshift, representing a ~52% complete sample over 0.28 deg². By its combination of angular coverage and high sampling rate, this survey provides the first detailed maps of the galaxy distribution in the redshift interval $0.1 \lesssim z \lesssim 0.5$. These maps reveal a large number of sharp walls separated by vast regions devoid of galaxies with diameters $\lesssim 50 \, h^{-1}$ Mpc (using $H_0 = 100 \, h$ km s^{-1} Mpc^{-1} and $q_0 = 0.5$). We find *no* evidence for periodic structure on scales ~130 h^{-1} Mpc as suggested by Koo et al. (1993). From the ESO-Sculptor Survey, the large-scale structure at $z \lesssim 0.5$ appears to be consistent with the results of the nearby surveys (Geller & Huchra 1989). These new data underline the essential role of densely sampled redshift surveys for understanding the large-scale clustering at large distances.

Subject headings: cosmology: observations — galaxies: distances and redshifts — large-scale structure of universe

1. INTRODUCTION

During the past 10 years, our understanding of the distribution of matter in the universe has evolved drastically. Three-dimensional maps of the galaxy distribution probing out to $z \sim 0.03$ and covering large solid angles on the sky show remarkable structures characterized by an alternation of large empty regions (~20–50 h^{-1} Mpc in diameter) with sharp walls of galaxies (de Lapparent et al. 1986; Haynes et al. 1988; Geller & Huchra 1989; da Costa et al. 1994). Recently, two wide-angle surveys at intermediate distances ($z \sim 0.2$; Shectman et al. 1992; Vettolani et al. 1993—see also Zucca et al. 1995) show similar structures to those detected in the nearby surveys, with typical void diameters $\lesssim 50 \, h^{-1}$ Mpc. In contrast, the deep pencil-beam survey of Broadhurst et al. (1990), which uses a collection of narrow probes to map the galaxy distribution to $z \sim 0.5$, shows an alternation of peaks and voids with a typical scale of 128 h^{-1} Mpc in the direction of the Galactic poles. This regularity is not confirmed in two other directions of the sky (Koo et al. 1993).

The presence of significant power on scales greater than 100 h^{-1} Mpc would put tight constraints on the theoretical models for the formation of large-scale structure and could call into question the models based on the gravitational evolution of Gaussian perturbations. These models support the observed cell-like pattern in the nearby distribution: for a Harrison-Zel'dovich fluctuation spectrum and $\Omega = 1$, the large-scale structure evolves into a void-filled universe with void sizes of ~60 h^{-1} Mpc (Piran et al. 1993). The high degree of isotropy of the microwave background radiation (Smoot et al. 1992) puts upper limits on the size of the underdense regions: only one structure with diameter 130 h^{-1} Mpc is expected within the whole Hubble volume (Blumenthal et al. 1992).

The variations in the detected structures from survey to survey demonstrate that the choice of the configuration of a survey, as defined by angular coverage, depth, and sampling

rate, determines its ability and efficiency to detect structure. For example, the sparse sampling rate in the survey by Koo et al. hinders the interpretation of the detected peaks and valleys in terms of walls and voids. The combination of sparse sampling and small-scale clustering can conspire to yield an artificial enhancement of the size and contrast of the detected structures (Ramella, Geller, & Huchra 1992; de Lapparent et al. 1991). The redshift survey of Willmer et al. (1994) having an overlapping area on the sky with the survey of Koo et al. (1993) and a higher sampling rate shows that intervening walls are missed in the survey by Koo et al. The objective-prism survey by Shuecker & Ott (1991), where the large errors in the velocities erase all structures on scales $\lesssim 30 \, h^{-1}$ Mpc shows *no* evidence for structure in the scale range 100–500 h^{-1} Mpc.

With the goal of mapping the large-scale structure at large distances and to reliably determine the typical and largest size of the structures, we started a fully sampled deep redshift survey over a substantial area of the sky. In this Letter we present the first results of the redshift survey obtained from the 52% complete partial data. In § 2 we define the data sample. In § 3 we describe the characteristics of the galaxy distribution in the survey. Section 4 summarizes and discusses the results.

2. THE DATA

The goal of the ESO-Sculptor Faint Galaxy Redshift Survey is to obtain a complete catalog of ~1000 galaxies with B, V (Johnson), R (Cousins) CCD photometry, along with spectroscopy and redshifts to a limit of $R \simeq 20.5$ in a 0.41 deg² region. The survey region has the configuration of a thin strip of 1°5 (R.A.) × 0°27 (decl.) and is centered near the southern Galactic pole in order to minimize the effects of Galactic extinction. The observations were performed using the 3.6 m telescope and the 3.5 m NTT (New Technology Telescope) at the European Southern Observatory (ESO). The photometric catalog derived from deep CCD images is complete to 24.5, 24, and 23.5 in B, V, and R, respectively. Spectra are obtained
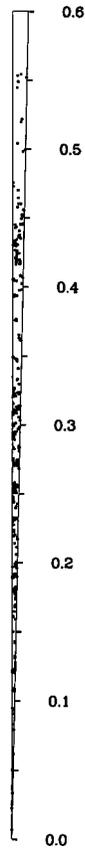
FIG. 1.—Cone diagram displaying redshift vs. R. A. for the 350 galaxies with $R \leq 20.5$ having a reliable redshift.

using multislit spectroscopy at a rate of ~30 objects per field of 35 arcmin^2 in ~2 hr of exposure time. The photometric and spectroscopic samples are described in detail by Arnouts et al. (1996) and by Bellanger et al. (1995), respectively.

To date, 514 spectra were observed and reduced over an area of ~0.28 deg^2 (~1°03 [R. A.] × 0°27 [decl.]). Reliable redshifts were derived for 353 galaxies with $R \leq 20.5$, representing a 52% complete sample over this area of the sky. The uncertainty in the redshifts varies between ~3×10^{-4} and 6×10^{-4} (~100–200 km s^{-1}).

3. THE LARGE-SCALE STRUCTURE

3.1. *Characteristic Pattern*

Figure 1 shows the map of the redshift distribution versus right ascension for 350 galaxies with $R \leq 20.5$ in the region defined by $0^h19^m \leq$ R. A. $\leq 0^h24^m$ and $-30°23 \leq$ decl. $\leq -29°95$ (J2000). The cone diagrams presented here (see also Fig. 2) have their true angular scale preserved (~1° in R. A.) in order to avoid introducing distortions into the three-dimensional shape of the detected structures. Figure 1 illustrates the large range of distances probed by the survey.

The galaxy distribution in Figure 1 is strongly clustered along the line of sight. Figure 2 provides a close-up view of the data by cutting the cone in Figure 1 into three chunks. The details of the spatial distribution show a striking alternation of voids and thin structures. Many of the intercepted structures of galaxies are remarkably sharp (at $z \sim 0.11$, 0.18, 0.19, 0.23, 0.29, 0.31), and some make a detectable angle with the

tangential direction (at $z \sim 0.18$, 0.29, 0.31). The typical diameter of voids as defined by the spacing between sharp structures appears to be in the range ~20–50 h^{-1} Mpc. These maps closely resemble the expected structure from an underlying distribution dominated by voids and walls of galaxies as those in the nearby surveys (Geller & Huchra 1989).

In contrast to the technique of sparsely sampling a wide region using many narrow pencil-beam probes (Koo et al. 1993; see discussion in §§ 3.3 and 4), the present survey provides a continuous transverse coverage of the intercepted structures over an intermediate area. At $z \sim 0.3$, the survey maps an area of 20 (R. A.) × 3.7 (decl.) h^{-2} Mpc^2 with $q_0 = 0.1$ and 13 (R. A.) × 3.5 (decl.) h^{-2} Mpc^2 with $q_0 = 0.5$ (this value is used throughout the paper unless otherwise specified). The largest transverse dimension of the survey is thus well above the correlation length, guaranteeing that the detected structures are not artifacts caused by small-scale clustering. Moreover, most of the sharp structures extend across the full survey area: displacements by $\lesssim 1°$ of the R. A. boundaries make no significant changes in the detected pattern, and the same large-scale structures are visible in the eastern and western parts of the cone diagram at nearly the same redshifts. This coherence of the intercepted structures is the characteristic signature of the large-scale walls of galaxies seen in the nearby surveys (Geller & Huchra 1989).

Other thin structures have a wide extent along the redshift direction ($\Delta z \sim 0.01$–0.02 at $z \sim 0.12$, 0.17, 0.22, 0.25, 0.42). However, the redshift extent of these structures is nearly an order of magnitude larger than the typical velocity dispersion for clusters of galaxies (Zabludoff, Huchra, & Geller 1990), and their projections on the sky have no clear density enhancement. These elongated structures are, therefore, either walls parallel to the line of sight, or complex structures made of small voids, or a combination of both. Using the estimate of the spatial density of clusters of galaxies from the survey by Mazure et al. (1995), 0.3 cluster with richness $R_{\rm ACO} \leq 1$ are expected within our survey volume of 4×10^4 h^{-3} Mpc^3, which explains why so few "fingers of god" are visible in Figure 2. Close examination of the map nevertheless reveals several poor "fingers" resembling groups of galaxies with $\lesssim 10$ members (at $z \sim 0.13$, $z \sim 0.23$, $z \sim 0.42$, and a pair of fingers at $z \sim 0.27$), as expected from the analysis of Ramella et al. (1989) which shows that groups populate regularly the large-scale walls.

Note that, although incomplete, the present subsample provides a fair representation of the geometry of the large-scale structure in this region of the sky. Its incompleteness is a slowly varying function with redshift that can only affect the relative density contrast of the walls. The coherence of the large-scale clustering in Figure 2 will then be strengthened when the redshift catalog is completed: the missing data is expected to populate the already detected walls and make them even denser (see Thorstensen et al. 1995).

3.2. *Peculiar Structures*

The maps in Figures 1 and 2 also contain some very large features which stand out clearly in the redshift distribution plotted in Figure 3: (1) a marked decrease in the galaxy density for $0.33 \leq z \leq 0.39$ (corresponding in comoving coordinates to ~200 h^{-1} Mpc with $q_0 = 0.1$ and ~170 h^{-1} Mpc with $q_0 = 0.5$); and (2) a broad peak centered at $z \sim 0.43$ and extended over ~100 h^{-1} Mpc. For comparison, the smooth curve in Figure 3
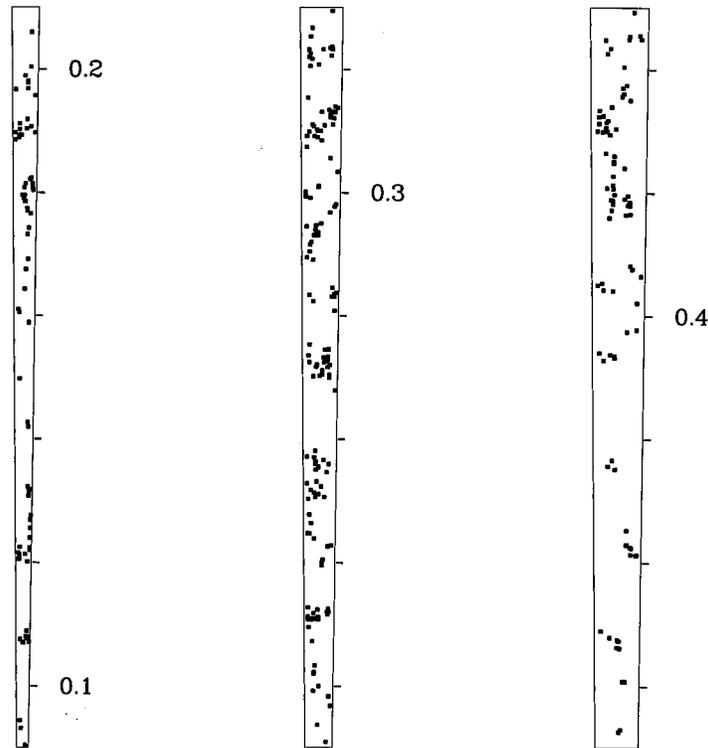
FIG. 2.—Close-up view of the redshift vs. R. A. cone diagram in Fig. 1. The first cone gives the distribution in the range $0.09 \leq z \leq 0.21$, the second in the range $0.21 \leq z \leq 0.33$, and the last in the range $0.33 \leq z \leq 0.45$. A total number of 318 galaxies with $R \leq 20.5$ and reliable redshifts are plotted.

gives the expected distribution for a no-evolution and spatially uniform model with correction for the varying incompleteness of the sample as a function of apparent magnitude (see Fig. 17 of Bellanger et al. 1995). The adopted luminosity function results from the combination of Schechter functions with parameters $M^* = -22.5$ and $\alpha = -1.1$ (and $H_0 = 75$ km s^{-1} Mpc^{-1}), and uses different K-corrections for the different morphological types (from Driver et al. 1994; we assume 30% of elliptical galaxies and 70% of spirals).
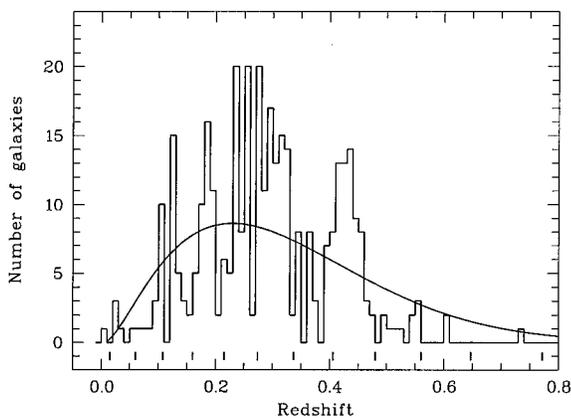

FIG. 3.—Observed redshift distribution for 353 galaxies with $R \leq 20.5$ in redshift increments of 0.01. The expected curve for a spatially uniform distribution is superposed (see text for details; the integrated count in the expected curve is normalized to the total number of observed galaxies). The thick vertical bars along the redshift axis correspond to the position of the 128 h^{-1} Mpc peaks of Koo et al. (1993) toward the southern Galactic pole.

These features correspond to respectively a strong deficit and excess of objects with respect to the expected curve. Comparison of the observed to expected number of objects in the redshift ranges of the underdense ($0.33 \leq z < 0.39$) and overdense ($0.41 \leq z < 0.46$) regions yield density contrasts N_{obs}/N_{exp} of $21/41 \simeq 0.5$ and $57/27 \simeq 2.1$, respectively. Galaxy clustering alone could be responsible for these deviations: under the assumption that the small- and large-scale clustering for the survey can be described by the canonical two-point galaxy correlation function (Maddox et al. 1990), the expected rms deviations in the number of objects contained within these respective regions are $N_{exp}^{1/2}(1 + N_{exp}\langle\xi\rangle)^{1/2} \simeq 10$ and 8, respectively ($\langle\xi\rangle = 0.04$ and 0.05, respectively).

Both features can be further explained in terms of accidental structure resulting from the combination of the sample shape with the complex nature of the large-scale clustering (highly asymmetric structures with varying galaxy density). Figure 2 shows that the underdense region contains tenuous structures of galaxies with similar separation as in the denser regions. The wide-angle surveys to nearby and intermediate distances indicate that the density of the large-scale walls varies spatially (Vogeley et al. 1994). The underdensity could, therefore, result from a chance alignment of several running portions of tenuous walls falling within the line of sight of our survey. The strong excess of galaxies at $z \sim 0.43$ in Figure 3 is partly caused by a wall of galaxies parallel to the line of sight: when plotting the redshift distribution in the restricted R. A. range 0^h21^m–0^h24^m, the peak in Figure 3 disappears. The probability to intersect a wall parallel to the line of sight becomes nonnegligible at large distance for our survey configuration.
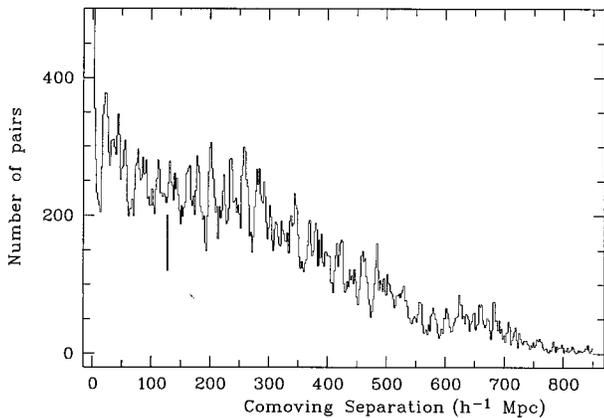
FIG. 4.—Distribution of line-of-sight pair separations for the 341 galaxies with $0.01 \leq z \leq 0.5$ in increments of $2\ h^{-1}$ Mpc. Comoving separations are derived using $q_0 = 0.5$.

3.3. *Typical Scales*

With the goal to measure quantitatively the characteristic size of the detected voids in Figure 2, we calculate the distribution of line-of-sight pair separations for the sample. Figure 4 shows the distribution in comoving coordinates for galaxies with $0.01 \leq z \leq 0.5$ in increments of $2\ h^{-1}$ Mpc. Confirming the visual impression given in Figure 2, the distribution shows a first peak centered at $22\ h^{-1}$ Mpc with a FWHM of $\sim 10\ h^{-1}$ Mpc. Using the approximation formulated by Szalay et al. (1991), which accounts for the excess variance due to small-scale clustering, the excess of pairs at $22 \pm 5\ h^{-1}$ Mpc is a 3.1 σ deviation. The rest of the pair distribution contains many peaks separated by 20–$30\ h^{-1}$ Mpc, as expected if the distribution is dominated by voids with a typical diameter. Note that the typical void size is probably underestimated as a given line of sight will rarely intercept a void through its center. Sophisticated analyses using simulated data with known topology are required in order to measure the characteristic size and properties of the voids intercepted by the survey.

Because our survey points $\sim 7°$ away from the southern probe of Koo et al. (1993), which corresponds to $\sim 100\ h^{-1}$ Mpc at $z = 0.3$ and might be close enough for coherent signal on scales $\gtrsim 100\ h^{-1}$ Mpc to propagate from one probe to another, it is informative to compare the two surveys. The scale of $128\ h^{-1}$ Mpc at which the signal is strongly periodic in the data by Koo et al. is indicated in the distribution of line-of-sight pair separations for our data (Fig. 4). In the data by Koo et al., there is a strong 4–$6\ \sigma$ peak at this scale (see Fig. 2a of Broadhurst et al. 1990). In our data, this scale falls in a dip of the distribution of line-of-sight pair separations. The neighboring peaks enclosed by the $1\ \sigma$ uncertainty in the $128\ h^{-1}$ Mpc scale ($\pm 10\ h^{-1}$ Mpc; Koo et al. 1993) are nonsignificant ($1.2\ \sigma$ at $112\ h^{-1}$ Mpc and $1.3\ \sigma$ at $132\ h^{-1}$ Mpc). There is thus no evidence in our data for a periodic pattern in the galaxy distribution on a scale of $128 \pm 10\ h^{-1}$ Mpc. This is also visible from the redshift distribution in Figure 3, which differs significantly from Figure 1 of Koo et al. For direct comparison of the detected structures in the two surveys, we plot in Figure 3 the positions of the $128\ h^{-1}$ Mpc peaks detected by Koo et al. toward the southern Galactic pole. Visual comparison shows

no obvious correlation between the peaks in our data and those from Koo et al. Quantitative prediction of the expected correlation between the two surveys requires a detailed analysis using simulated data sampled by neighboring lines of sight.

4. SUMMARY AND DISCUSSION

In order to determine the characteristics of the distribution of galaxies at large scale, we are performing a fully sampled faint galaxy redshift survey to $R \leq 20.5$. The observed region is located near the southern Galactic pole and has the configuration of a thin strip of $1°.0 \times 0°.27$. The map of the galaxy distribution for the 353 available redshifts (a 52% complete sample) is dominated by a regular pattern of large voids and sharp structures analogous to the Great Wall (Geller & Huchra 1989). The two large density fluctuations detected in the redshift range 0.3–0.5 could result from the combination of sample shape with the complex large-scale structure pattern. The distribution of line-of-sight pair separations exhibits a first peak at $22 \pm 5\ h^{-1}$ Mpc corresponding to a 3.1 σ excess of pairs, followed by a large number of peaks separated by ~ 20–$30\ h^{-1}$ Mpc. This analysis provides an estimate of the typical void size which is in good agreement with the results from void statistics applied to the CfA Redshift Survey (Vogeley, Geller, & Huchra 1991) and more generally with the range of void diameters measured in the various wide-angle surveys (20–$50\ h^{-1}$ Mpc). The ESO-Sculptor Survey thus provides the first evidence that the large-scale structure at large distances ($z \lesssim 0.5$) has similar properties to the nearby large-scale structure.

Another significant result of the new data presented here is that they contain no evidence for a periodic signal on a scale of $\sim 128 \pm 10\ h^{-1}$ Mpc as detected by Koo et al. (1993). Moreover, there is no apparent correlation between the redshift distribution in our survey and the peaks detected by Koo et al. in their southern probe pointing $7°$ away from our survey (i.e., $\sim 100\ h^{-1}$ Mpc at $z \sim 0.3$). This discrepancy between our results and those of Koo et al. is symptomatic of the difference of strategy used in the two surveys. Our available data represents a 52% complete sample of a contiguous $1°$ strip of the sky. The southern probe of Koo et al. corresponds to ~ 10 small probes of $10'$–$40'$ in diameter distributed over an $8° \times 8°$ region of the sky (Szalay 1993). Using the ratio of the number of measured redshifts to the expected total number of galaxies in this area, we estimate that their overall sampling rate is $\lesssim 2\%$. Figure 1a of Broadhurst et al. (1992) illustrates that this low sampling rate is insufficient for mapping the detailed large-scale structure; in this map, the correspondence between the $128\ h^{-1}$ Mpc peaks and the large-scale structure is unclear, raising questions on the nature of the peaks. The new data presented here demonstrate the importance of a high sampling rate for reliable detection of the dominant large-scale features. The ESO-Sculptor Survey was designed to reliably detect structures similar to those seen in the CfA Redshift Survey and it succeeds in this task.

New spectra are being reduced and will bring the $1° \times 0°.27$ strip to a redshift completeness of 80%–100%. Additional data which should increase the survey area to a $1°.5 \times 0°.27$ strip were obtained in the fall of 1995. These new data will be crucial for confirming the preliminary results presented here and for clear understanding of the nature of the clustering in this region of the sky. Detailed statistics will be used on the completed data in order to determine the typical properties of

the large-scale clustering at $z \sim 0.1$–0.5 on scales of ~ 20–100 h^{-1} Mpc (void probabilities; genus analyses; wavelet analysis; etc., ...). The power spectrum will also be essential for estimating the amount of clustering on scales $\gtrsim 100$ h^{-1} Mpc, which are well sampled by the long line of sight of the survey (~ 1100 h^{-1} Mpc at $z \sim 0.5$). As a unique database by its combination of spectroscopy and multicolor CCD imaging, the ESO-Sculptor Survey will also allow us to study how the local galaxy density and the location within the large-scale struc-tures affect the morphological and spectrophotometric prop-erties of galaxies.

REFERENCES

Arnouts, S., de Lapparent, V., Mathez, G., Mazure, A., Mellier, Y., Bertin, E., & Kruszewski, A. 1996, A&A, in press
Bellanger, C., de Lapparent, V., Arnouts, S., Mathez, G., Mazure, A., & Mellier, Y. 1995, A&AS, 110, 159
Blumenthal, G. R., da Costa, L. N., Goldwirth, D. S., Lecar, M., & Piran, T. 1992, ApJ, 388, 234
Broadhurst, T. J., Ellis, R. S., Koo, D. C., & Szalay, A. S. 1990, Nature, 343, 726
———. 1992, in Proc. Digitized Optical Sky Surveys, ed. H. T. MacGillivray & E. B. Thomson (Dordrecht: Kluwer), 397
da Costa, L. N., et al. 1994, ApJ, 424, L1
de Lapparent, V., Geller, M. J., & Huchra, J. P. 1986, ApJ, 302, L1
———. 1991, ApJ, 369, 273
Driver, S. P., Phillipps, S., Davies, J. I., Morgan, I., & Disney, M. J. 1994, MNRAS, 266, 15
Geller, M. J., & Huchra, J. P. 1989, Science, 246, 897
Haynes, M. P., & Giovanelli, R. 1988, in Large-Scale Motions in the Universe, ed. V. C. Rubin & G. V. Coyne (Princeton: Princeton Univ. Press), 31
Koo, D. C., Ellman, N., Kron, R. G., Munn, J. A., Szalay, A. S., Broadhurst, T. J., & Ellis, R. S., 1993, in ASP Conf. Ser. 51, Observational Cosmology, ed. G. Chincarini, A. Iovino, T. Maccacaro, & D. Maccagni (San Francisco: ASP), 112
Maddox, S. J., Efstathiou, G., Sutherland, W. J., & Loveday, J. 1990, MNRAS, 242, 43P
Mazure, A., et al. 1995, A&A, in press

Piran, T., Lecar, M., Goldwirth, D. S., da Costa, L. N., & Blumenthal, G. R. 1993, MNRAS, 265, 681
Ramella, M., Geller, M. J., & Huchra, J. P. 1989, ApJ, 344, 57
———. 1992, ApJ, 384, 396
Schuecker, P., & Ott, H. A. 1991, ApJ, 378, L1
Shectman, S. A., Schechter, P. L., Oemler, A., Jr., Tucker, D., Kirshner, R. P., & Lin, H. 1992, in Clusters and Superclusters of Galaxies, ed A. C. Fabian (Dordrecht: Kluwer), 351
Smoot, G. F., et al. 1992, ApJ, 396, L1
Szalay, A. S. 1993, Ecole de Physique Théorique des Houches
Szalay, A. S., Ellis, R. S., Koo, D. C., & Broadhurst, T. J. 1991, in AIP Conf. Proc. 222, After the First Three Minutes, ed. S. S. Holt, C. L. Bennett, & V. Trimble (New York: AIP), 261
Thorstensen, J. R., Kurtz, M. J., Geller, M. J., Ringwald, F. A., & Wegner, G. 1995, AJ, 109, 2368
Vettolani, G., et al. 1993, in Proc. 9th IAP Meeting, Cosmic Velocity Fields, ed. F. R. Bouchet & M. Lachièze-Rey (Gif-sur-Yvette: Editions Frontières), 523
Vogeley, M. S., Geller, M. J., & Huchra, J. P. 1991, ApJ, 382, 44
Vogeley, M. S., Park, C., Geller, M. J., Huchra, J. P., & Gott, J. R., III. 1994, ApJ, 420, 525
Willmer, C. N. A., Koo, D. C., Szalay, A. S., & Kurtz, M. J. 1994, ApJ, 437, 560
Zabludoff, A. I., Huchra, J. P., & Geller, M. J. 1990, ApJS, 74, 1
Zucca, E., et al. 1995, in Proc. XVth Moriond Astrophysics Meeting, Clustering in the Universe (Gif-sur-Yvette: Editions Frontières), in press